

REVIEW ARTICLE OPEN



Protein-based antigen presentation platforms for nanoparticle vaccines

Brian Nguyen¹ and Niraj H. Tolia¹✉

Modern vaccine design has sought a minimalization approach, moving to the isolation of antigens from pathogens that invoke a strong neutralizing immune response. This approach has created safer vaccines but may limit vaccine efficacy due to poor immunogenicity. To combat global diseases such as COVID-19, malaria, and AIDS there is a clear urgency for more effective next-generation vaccines. One approach to improve the immunogenicity of vaccines is the use of nanoparticle platforms that present a repetitive array of antigen on its surface. This technology has been shown to improve antigen presenting cell uptake, lymph node trafficking, and B-cell activation through increased avidity and particle size. With a focus on design, we summarize natural platforms, methods of antigen attachment, and advancements in generating self-assembly that have led to new engineered platforms. We further examine critical parameters that will direct the usage and development of more effective platforms.

npj Vaccines (2021)6:70; <https://doi.org/10.1038/s41541-021-00330-7>

INTRODUCTION

The term “nanoparticle” has varied usage in the scientific literature. For biological products the United States Food and Drug Administration (FDA) classifies a nanoparticle as a material or substance that has been deliberately manipulated to have dimensions between 1 to 100 nm or up to 1000 nm if it exhibits physical, chemical, or biological effects dependent on its size¹. Particles in this size range can significantly influence biological systems, driving the expansion of nanoparticle research in biology and medicine. In vaccinology, nanoparticles serve three major roles: as adjuvants, carriers, or presentation platforms, determined by how the vaccine antigen interacts with the nanoparticle (Fig. 1)². Upon vaccination, a nanoparticle is used to improve the immune response through one or a combination of these roles. Nanoparticles have demonstrated remarkable success as particulate adjuvants^{2,3} and nucleic acid delivery carriers⁴, however, this review will specifically focus on protein-based nanoparticle platforms. Previous publications have summarized the characteristics, utilization, and efficacy of nanoparticle platforms in vaccines^{2,5–8} and the bioengineering strategies^{9–13} of self-assembling proteins applicable for the design of new potential platforms. This review serves to provide an updated, comprehensive and concise analysis on current platforms, the design strategies for novel platforms, and how the structural characteristics of these platforms affect the immune response at the molecular level.

Nanoparticle platforms in vaccine development

Nanoparticle platforms involve the attachment of antigen to the surface of a particle, either inorganic or organic in nature, (Fig. 1) to promote an immune response through enhanced trafficking and recognition by cellular receptors. Inorganic platforms raise concerns of toxicity and non-biodegradability. Micellar platforms, which have been used to present SARS-CoV-2 Spike trimers, may be limited to antigens with a transmembrane domain¹⁴. In contrast, protein-based platforms are highly biocompatible, can assemble homogeneously, and can be effectively tailored to suit

any antigen. Protein nanoparticles injected intravenously have been shown to freely travel through circulatory and lymph vessels with rapid accumulation in the thyroid and spleen, advantageous for establishing humoral immunity¹⁵. Furthermore, protein-based platforms enable antigen attachment through genetic fusion or affinity tags complexes, which allows for a homogenous decoration of antigens on the platform. The first protein platforms utilized virus capsid proteins isolated from their infectious components and exploited their naturally oligomeric nature to form stable nanoparticles called virus-like-particles or VLPs⁵. Subsequently, many naturally oligomeric proteins such as ferritin, lumazine synthase, and C4b-binding protein (C4bp) orthologs have been developed for platform design. These platforms vary in size, ranging from as little as 4 nm with C4-binding protein-like particles to as large as 120 nm with Influenza M1 VLPs⁶ (Table 1). Recent advances in computational protein design have enabled development of synthetic platforms, where pre-existing proteins are engineered to assemble into highly oligomeric complexes, which rival naturally occurring platforms in size and antigen valency.

Protein nanoparticle platforms improve the immune response to antigens in vaccines

The effectiveness of a prophylactic vaccine is determined by the generation of a long-lasting T-cell-dependent IgG antibody response¹⁶. Generating this response involves the activation of T-cells by antigen presenting cells (APC) followed by the activation of B-cells by antigen and a specialized T helper cell, the T Follicular helper (T_{FH})¹⁷. APCs phagocytize, process, and present antigens to T-cells, which if recognized, become activated to differentiate into T helper cells. Naive B-cells, which require two signals to mature into high-affinity IgG plasma cells, receive the first signal from the crosslinking of multiple B-cell receptors (BCR) with an antigen that has directly entered the lymph node or was presented by APCs, followed by endocytosis of the receptor and antigen, and then presentation of the processed antigen on the surface. The second signal is delivered upon recognition of the B-cell-presented

¹Laboratory of Malaria Immunology and Vaccinology, National Institute of Allergy and Infectious Diseases, National Institute of Health, Bethesda, MD, USA. ✉email: niraj.tolia@nih.gov

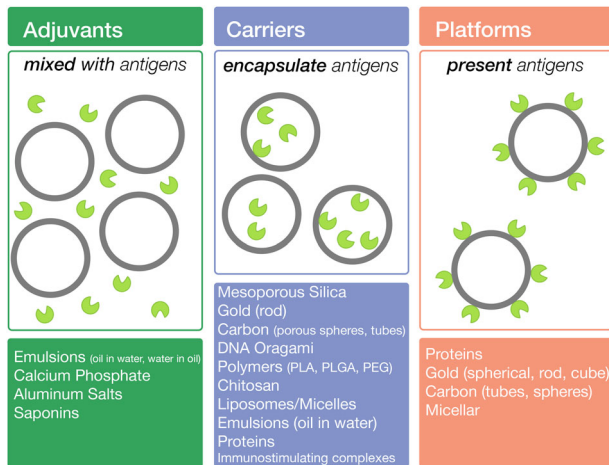


Fig. 1 The three categories of nanoparticle roles in vaccines as adjuvants, carriers, and platforms with the descriptions of the role below. Gray circles represent nanoparticles while, green circular indented units represent antigens. Abbreviations PLA, PLGA, and PEG correspond to polylactic acid, polylactic-co-glycolic acid, and polyethylene glycol, respectively. Modified and adapted from Zhao et al.².

Table 1. Structural comparison of different self-assembling proteins; size was measured from the longest axis while # subunits indicate the number of monomers within the nanoparticle. Fused subunits are counted as one monomer.

Name	Size (nM)	MW (kDa)	# Subunits	PDB	References
IMX313	4.4	150	7	4B0F	45
Nsp10	8.4	204	12	2G9T	72
T3 (10)	11	276	12	4DCL	77
T32 (28)	11	571.8	24	4NWN	78
Ferritin	12	456	24	1AEW	64
T33 (15)	12.2	406.8	24	4NWO	78
O3 (33)	13	478.8	24	3VCD	77
Lumazine Synthase	15	1002.6	60	1HQK	69
T3 + 2	16	602.64	12	3VDX	76
O3 + 4CC	18	886	24	n/a	80
HbsAg VLP	22	3076.9~	96~	n/a	50
O3 + 2	22.5	750	24	n/a	79
E2p	23.2	1595.8	60	1B5S	71
I3 (01)	25	1432.8	60	1VLW*	82
I3 + 5CC	25	2167.8	60	n/a	81
I52 (32)	25.3	1993.8	120	5IM4	83
AP205 VLP	27.2	2520	180	5LQP	59,60
I53 (50)	27.5	2479.2	120	EMD-0350 (Cryo-EM)	83
I32 (28)	28.6	2053.2	120	5IM6	83
Ico532-1	30	2520	60	n/a	84
M1 VLP	120	~	~	n/a	6

Asterisk (*) indicates that the engineered nanoparticle structure was not available and a PDB structure of the original building block was provided instead. Tilde (~) indicates that value may vary due to lipid composition.

antigen with a T_{FH} cell, which activates the B-cell to mature into an IgG-producing plasma cell.

Many successful vaccines in the past consisted of attenuated vaccines that were highly effective but were potentially infectious. This deficiency prompted the creation of inactivated components or subunit vaccines, for example those used in modern influenza vaccines. Subunit vaccines typically have excellent safety profiles by consisting of isolated antigens necessary to establish an immune response, and as a result may also be less immunogenic. However, vaccination with certain subunit vaccines such as those against Human papillomavirus (HPV), Cervarix and Gardasil, has seen remarkable success in protection¹⁸. This success has been attributed in part to the ability of the antigen, the major capsid protein, to self-assemble into highly oligomeric spherical VLPs. However, many antigens, such as those used in influenza subunit vaccines, do not self-assemble into nanoparticles. In these cases, self-assembly can be generated by attachment of these antigens to an oligomeric protein platform. Studies have shown that scaffolded antigen induce stronger and longer lasting neutralizing antibody titers, as well as greater protection^{19–24}.

Two characteristics of nanoparticle platforms contribute to generating the B-cell IgG response: (1) the attachment of the antigen to a larger scaffold, which improves APC uptake and retention in lymph follicles and (2) the repetitive array of antigens, which enables efficient binding and activation of multiple B-cell receptors (Fig. 2). Attachment of antigens on particles increases the overall particulate size into an optimal size range for efficient uptake by APCs, which allows for greater presentation of antigen by APCs to activate T-helper cells^{25,26} (Fig. 2a). Larger particles are also efficiently opsonized with complement²⁷. Opsonization promotes binding to the surface of FDCs (follicular dendritic cells), elongating retention in lymph follicles, and enhancing antigen presentation to B-cells²⁷. Particles displaying numerous antigens can then facilitate B-cell activation through efficient crosslinking with multiple BCRs^{26,28} (Fig. 2b). Evidence of this claim is demonstrated by one study that examined how the density of an antigen, a model peptide, affected memory immune response²⁹. High-density conjugation of an antigen to a VLP activated a specific IgG antibody response, while low-density conjugation did not (despite increased antigen quantity), suggesting an effect outside the total amount of antigen. In addition to enhanced B-cell activation caused by repetitive antigen surfaces, the immune system appears to be trained to recognize these surfaces, such as viral capsids and bacterial pili, as a non-self indicator^{28,30}. Because of this effect, protein platforms have enabled self-antigen, that are normally dispersed, to break self-tolerance and mount an immune response³¹. The ability to break self-tolerance has facilitated the use of protein platforms in cancer vaccine development through the presentation of tumor-associated antigens (TAAs), which are self-antigens overexpressed in cancerous tissue but rarely observed in normal tissue³¹.

Protein nanoparticles can help in the development of vaccines for immuno-evasive pathogens such as human immunodeficiency virus (HIV), influenza, and malaria⁵. Antibody-dependent-enhancement (ADE), which contributes to the infection of HIV and Dengue, occurs when non-neutralizing antibodies bind and encourage infection of immune cells³². To counter this possibility a technique called epitope focusing has been used to design antigens that direct an antibody response to neutralizing epitopes. This technique that involves isolating neutralizing epitopes from antigens are oftentimes poorly immunogenic in isolation. However, when attached to a nanoparticle platform, the increased presentation allows these antigens to yield a strong yet targeted humoral response³³. In addition to epitope focusing, T-cell epitopes introduced in the interior of the platform can be used to activate a cell-mediated immune response^{34,35}. Incorporation of universal CD4 + T-cell epitopes can help establish a humoral response against the antigen through recruitment of helper-T cells

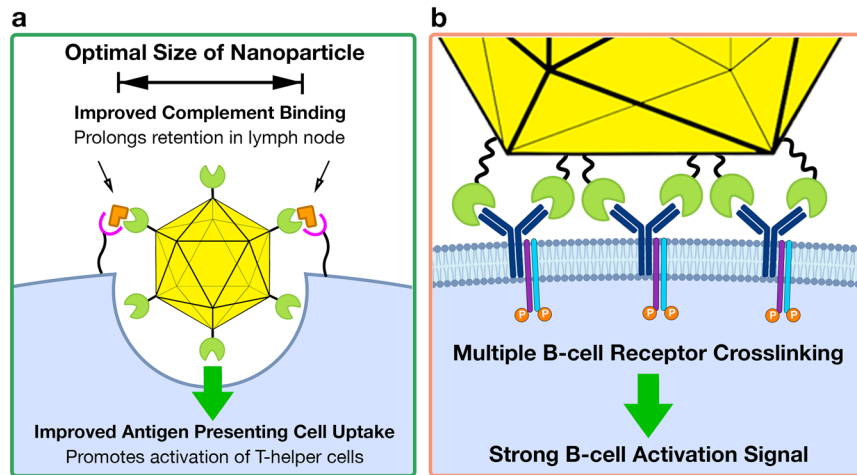


Fig. 2 Advantages of protein nanoparticle vaccines. Yellow icosahedrons represent a protein nanoparticle platform while green circular sectors represent a genetically fused antigen. **a** Beneficial effects of increased size by presenting antigen on a nanoparticle platform. One of these effects is improved binding of complement indicated by the rectangular orange shape, on the surface of the nanoparticle. The bound complement facilitates binding to complement receptors on APCs such as follicular dendritic cells and promotes retention of the opsonized nanoparticles in the lymph nodes. Another effect of increased size is enhanced uptake of nanoparticles by APCs, indicated by the circular cavity and direction of travel arrow into the APC, in light blue. **b** Enhanced B-cell activation through the interaction of multiple antigens with BCRs, which are embedded within the membrane of the B-cell.

while CD8 + T-cell epitopes can generate killer T-cells against a specific pathogen. The combination of these techniques may enable successful vaccination against difficult pathogens.

Antigen attachment

Three different methods are used to attach antigens for presentation on nanoparticles: chemical conjugation, genetic fusion, and tag coupling (Fig. 3). These methods allow platforms to be decorated with numerous antigens, resulting in increased presentation and size. Conjugation relies on chemical treatment to crosslink antigens to the platform, which can lead to an uneven decoration. The other methods, such as genetic fusion and tag coupling, attach antigen specifically to the terminals and offer a more precise antigen arrangement.

In a typical chemical conjugation used for antigen attachment to VLPs, the protein nanoparticle undergoes chemical treatment to crosslink surface-exposed lysines to engineered or surface-exposed cysteines of a target antigen³⁶ (Fig. 3a). This method has seen success in licensed *Haemophilus influenzae* type b (Hib) vaccines³⁷, which conjugates polysaccharides of Hib to an immunogenic protein platform such as Tetanus toxoid. The established nature of this method has led researchers to explore vaccines that use conjugation to attach protein-based antigen. Decoration of *Pseudomonas aeruginosa* exoprotein A (EPA), an inherently immunogenic protein, with a malaria antigen has led to a 75- to 110-fold increase in specific antibody generation versus immunization without EPA^{38–40}. For this case the antigen was lysine-treated and conjugated to the cysteine of EPA⁴¹. Unlike other methods, conjugation can be used to decorate monomeric proteins with numerous antigens. However, the uneven decoration of this method may lead to poor display of antigen and inefficient B-cell activation against neutralizing epitopes⁴². Nevertheless, chemical conjugation has been proven to significantly improve immune responses despite these supposed limitations.

Genetic fusion and tag coupling can often provide greater precision through site-specific antigen attachment. Genetic fusion of the antigen to the nanoparticle platform is the most direct method (Fig. 3b) if the appropriate terminal on the nanoparticle, depending on the antigen's own terminals, is accessible and properly orients the antigen. However, there are some cases where separate expression and purification of the antigen and

platform may be preferred, such as when fused constructs do not express properly or inhibit proper folding of the nanoparticle. Tag-coupling systems allow for independent expression and modular attachment of antigens, although they still require some genetic fusion (Fig. 3c). Most tag-coupling scenarios involve the binding of a tag, which is fused to a terminus on one protein, to a protein receptor or catcher, which is fused to the partner protein. Popular tag-coupling systems include Biotin-Avidin, HaloTag, and SpyTag/SpyCatcher³⁶.

SpyTag/SpyCatcher has had the most extensive use in antigen presentation platforms^{20,42–44}. This system uses *Streptococcus pyogenes* fibronectin-binding protein FbaB, which has been split in two components, SpyCatcher (113 aa) and SpyTag (13 aa). Nanoparticle platforms that are fused to a SpyCatcher form an irreversible peptide bond with the SpyTag fused to the antigen or vice versa and can be fused to either the N- or C-terminal. Attachment of two different antigens can be accomplished by combining SpyTag/SpyCatcher with another tag-coupling system such as SnoopTag/SnoopCatcher⁴⁵. Tag coupling can result in a lower numbers of antigen per particle than genetic fusion, due to inefficient coupling⁴⁶. In addition, the genetic fusion of a large protein (e.g., SpyCatcher) to the nanoparticle may interfere with the attachment of antigen. Ultimately, tag-coupling systems allow for rapid modular attachment of different antigens to a nanoparticle platform, at the cost of introducing more components.

Natural nanoparticle platforms: virus-like particles (VLPs)

Virus-like particles (VLPs) are composed of self-assembling viral envelope or capsid proteins, ranging from 20 nm to 800 nm in diameter (Table 1), which are devoid of any infectious component². VLPs were the first nanoparticles to be used in vaccines due to the relative ease of design that exploited naturally high stability and self-assembly. VLPs have seen extensive use in clinical trials and commercially approved vaccines as platforms and demonstrate a reliable proof-of-principle for protein platform technology.

The world's first licensed and approved malaria vaccine, RTS,S, is based on VLPs⁴⁷. RTS,S uses the hepatitis B virus surface antigen small-envelope protein (HbsAg) to self-assemble into a spherical nanoparticle⁴⁸. HbsAg, which is the main component in currently approved hepatitis B vaccines⁴⁹, forms the lipid viral envelope that

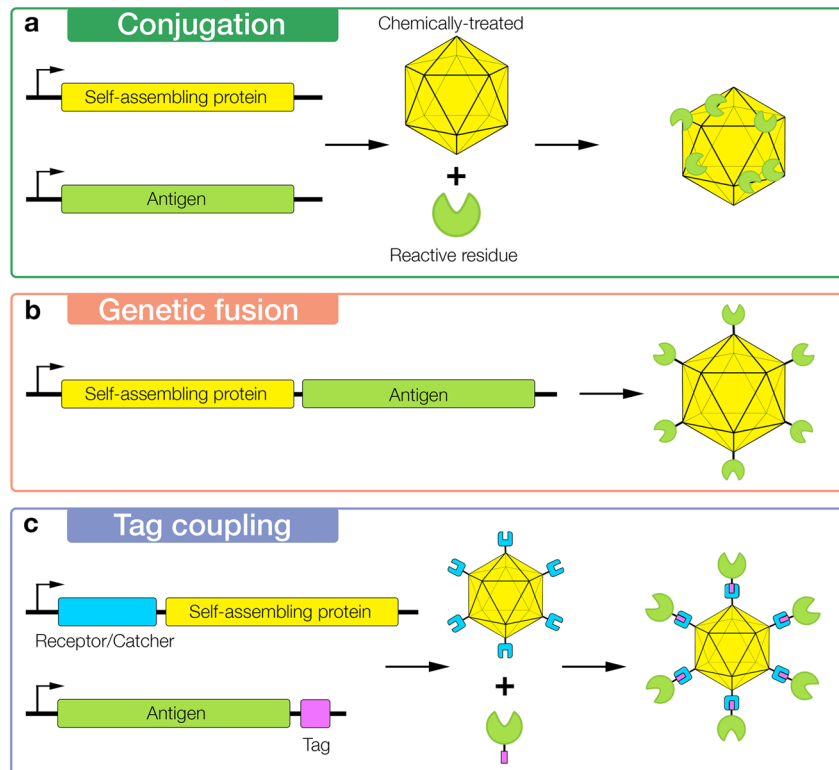


Fig. 3 Methods of Antigen attachment to nanoparticle platform. Protein sequences are indicated by rectangular boxes, arranged left to right from N to C terminals. Protein nanoparticle platforms are represented by a yellow icosahedron and antigens are represented as a green circular sector. **a** A typical chemical conjugation scheme for protein nanoparticles, which involves the chemical treatment of a reactive amino acid on either the nanoparticle or antigen to conjugate with a reactive amino acid on the other respective protein. In this case, the nanoparticle is chemically treated to bind with a reactive amino acid residue on the antigen. **b** Genetic fusion with the platform, indicated by a distinct black line between the antigen and nanoparticle. **c** An example of tag-coupling systems, where the genetic fusion of a protein receptor or protein catcher, represented as cyan colored squares with a cavity, to one component allows for binding to another component through a genetically fused tag, represented as a small pink rectangle.

encloses the capsid and is able to form noninfectious particles 22 nm in diameter⁵⁰. Further structural characterizations suggests that an HbsAg VLP consists of 24 tetramers, with a rhombicuboctahedron-like shape, although exact composition may vary due to lipid nature⁵¹. Antigen attachment to the envelope in RTS,S is accomplished by genetic fusion of a malaria antigen to the N-terminus of HbsAg⁴⁸. The fused HbsAg is then coexpressed with unmodified HbsAg to allow for nanoparticle formation, although nanoparticles consisting solely of fused HbsAg have also been created⁵². Vaccination with RTS,S confers moderate protection against malaria, and attachment of the antigen to the VLP has been credited with significantly increasing its efficacy⁵³.

Influenza Matrix 1 (M1) protein-based VLP is a second enveloped VLP platform, which has seen usage in clinical trials for an influenza vaccine⁵⁴. This platform forms large spheroid particles around 120 nm in diameter⁵⁵. To assemble into VLPs M1 must interact with proteins containing a cytoplasmic tail region such as HA (hemagglutinin) and NA (neuraminidase)⁵⁶. M1 VLPs have been made with different combinations of influenza surface glycoproteins or envelope proteins from other viruses and has been expressed in mammalian and insect systems^{57,58}. M1 VLPs were used in a SARS-CoV vaccine, consisting of M1 envelope protein and chimeric spike protein¹⁹. Replacement of the spike protein transmembrane and C-terminus regions with those of HA allowed the antigen to insert itself into the lipid membrane formed by the envelope protein. Vaccination of mice with the chimeric spike VLP protected mice against SARS-CoV.

Comparatively, vaccination with spike alone required the addition of adjuvant for protection.

Capsid VLPs based on bacteriophage AP205 coat protein have shown relative ease of antigen attachment⁵⁹. In contrast to enveloped VLPs that incorporate a lipid membrane, capsid-based VLPs are completely composed of protein. 180 monomers of the coat protein oligomerize to form a capsid that resembles a truncated icosahedron with 20 hexameric facets and 12 pentameric vertices (Fig. 4)⁶⁰. The coat protein exists primarily as dimers and five dimers form the pentameric vertices while six dimers form the hexameric facets. The dimers are interwoven between adjacent pentameric vertices or hexameric facets. The N- and C-termini of the coat protein are located close to the threefold axis of the hexameric facets, allowing for ideal attachment of trimeric antigens to either terminus. Attachment of a host self-antigen to AP205 elicited a highly immunogenic response that overcame B-cell unresponsiveness to self-antigens⁵⁹, demonstrating the effectiveness of nanoparticle presentation. In another study, a lysine and cysteine-rich Inter-Domain Region (CIDR) antigen from *P. falciparum* erythrocyte membrane protein 1 (PfEMP1) was attached to AP205 with the Spyttag-Spycatcher coupling system²⁰. AP205 coupled with CIDR produced significantly higher antibody titers after immunization in mice versus non-coupled AP205 & antigen or antigen alone. As a cancer vaccine, AP205 elicited an auto-antibody response against human epidermal growth factor receptor-2 through genetic fusion to the AP205 VLP⁶¹.

VLPs have demonstrated remarkable improvements in improving the humoral immune response when used as a platform for antigens. However, VLPs can be difficult to produce due to low

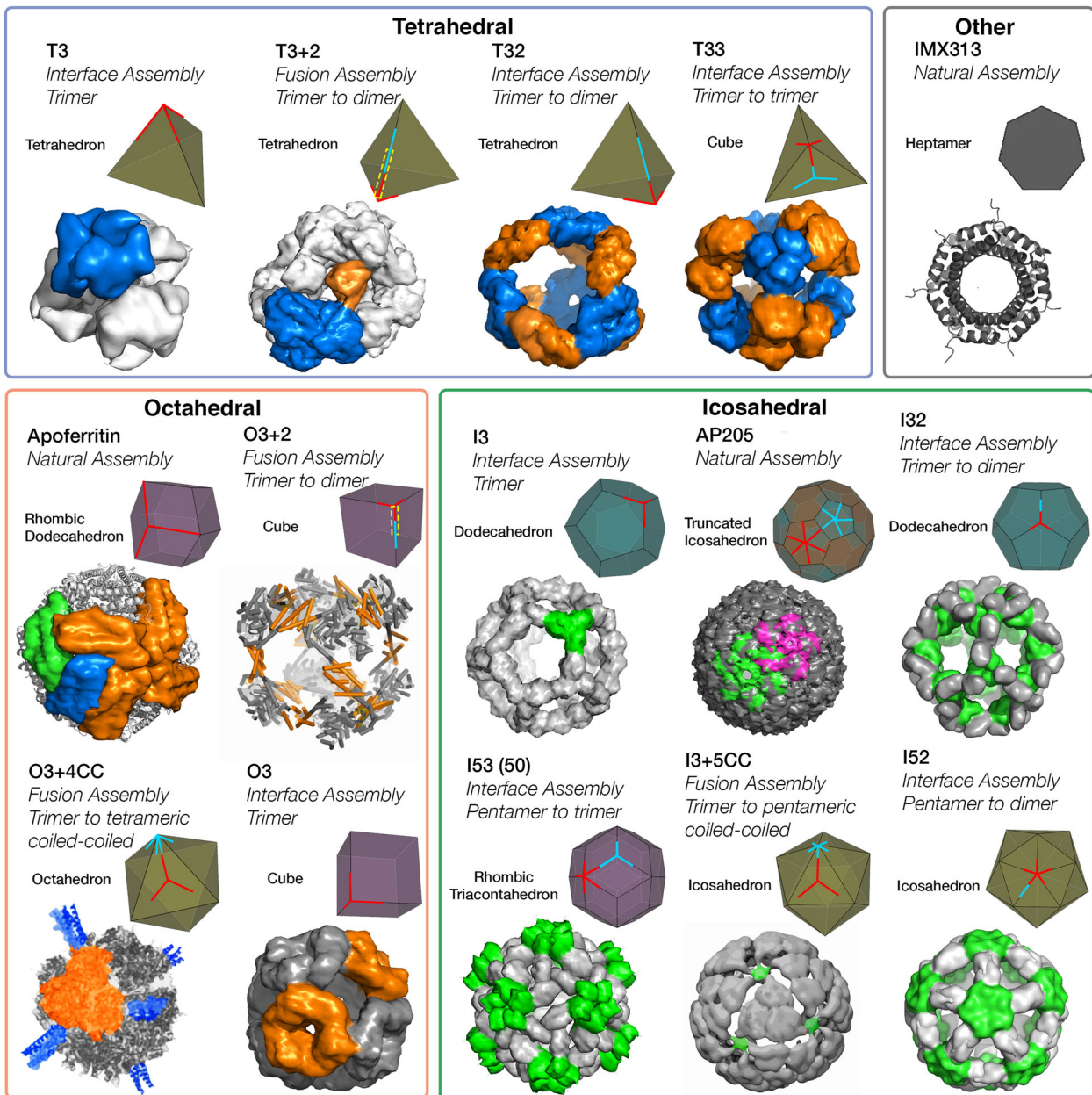


Fig. 4 Summary of published engineered self-assembling nanoparticles and naturally assembling nanoparticles, sorted by symmetry type. For the names of engineered nanoparticles, the first letter indicates symmetry of the design T, O, or I for tetrahedral, octahedral, icosahedral, respectively. The first number indicates the oligomeric state of the primary building block, while the second number represents the oligomeric state of the secondary building block, if present in the design. The abbreviation “CC” stands for a coiled-coil motif. A plus (+) between the first and second number indicates that self-assembly is generated by genetic fusion between two monomers of the primary and secondary building block, versus Interface design with Rosetta. As a visual aid, the primary building block (red) and secondary (cyan) are aligned to the vertices or faces of a polyhedra^{98,99} that resembles the geometry of the nanoparticle. Genetically fused building blocks are emphasized with a yellow-dashed box.

expression yields and the presence of host cell contaminants from expression systems⁶². VLPs assembled *in vivo* can encapsulate host DNA and other host proteins, potentially due to their nature, which encourages the packaging of genomic information. Removal of such contaminants involves complex purification or *in vitro* disassembly and reassembly steps⁶². VLPs also suffer from stability issues, possibly due to a lack of viral genome⁶³. Additionally, enveloped VLPs require eukaryotic host expression systems in order to acquire their lipid membrane. VLPs are well-established, however, manufacturing complications hinder their adoption as platforms.

Nanoparticle platforms: non-VLP self-assembling proteins

As an alternative to VLPs, non-viral proteins that are highly oligomeric have been used as platforms. These platforms are often enzymes or homeostasis proteins that can be easily produced. A hallmark of self-assembling proteins is a single protein component that readily assemble into stable highly oligomeric structures that complement icosahedral VLPs.

A popular non-viral platform is Ferritin, a protein involved in intracellular iron storage that is found in nearly all organisms and consists of 24 monomers with a molecular weight of 18 kDa each⁶⁴. The complex consists of 8 trimers with octahedral

symmetry and resembles a rhombic dodecahedron: a polyhedron with both threefold and fourfold symmetry⁶⁴ (Fig. 4). The close proximity of the N-termini to the threefold axis allows for easy attachment of trimeric antigens. In contrast, the C-terminus is buried and unavailable for antigen presentation. Mammalian expression systems have been the standard for ferritin-based vaccines, although *E. coli* expression and refolding has also been examined^{65,66}. *Helicobacter pylori* ferritin has been commonly used in vaccine design due to its sequence divergence from human ferritin; when fused to HA, *H. pylori* ferritin elicited antibody protection against influenza with greater potency than commercial influenza vaccines⁶⁷. A two-component dual-antigen ferritin derived from *Trichoplusia ni* has also been produced, and elicited neutralizing antibodies against both targets⁶⁸. A recent study has successfully presented SARS-CoV-2 trimers fused with a C-terminal SpyCatcher on ferritin with a N-terminal SpyTag using a mammalian secretion expression system⁴⁶. Addition of N-linked glycosylation sites to the nanoparticle improved expression yield. Successful presentation of trimers was indicated by binding to SARS-CoV-2 antibodies. Ferritin is a robust and well-established platform that provides a natural alternative to VLPs. However, ferritin is also significantly smaller and contains less subunits than VLPs (Table 1).

Lumazine synthase (LS), an enzyme involved in riboflavin synthesis, is an icosahedral non-VLP platform that has significantly more subunits than ferritin. Sixty monomers of pentameric protein naturally assemble into particles resembling a dodecahedron⁶⁹. Both N- and C-termini of LS are surface-exposed and contain threefold and fivefold symmetry, although the N-terminus appears to be closer to the threefold apex than the C-terminus. The proximity of the termini to the symmetry axis may stabilize the presentation of trimeric or pentameric antigens. Genetic fusion of a trimeric HIV surface antigen (gp120), which was truncated and stabilized with a coiled-coil linker to the C-terminus of LS from *Aquifex aeolicus* significantly improved B-cell activation compared to antigen alone²¹. Similar to ferritin, LS has also successfully presented SARS-CoV-2 trimers on LS with a similar construct design, glycosylation modifications, and expression system used for ferritin⁴⁶. LS is typically expressed in a mammalian cell secretion system, although *E. coli* expression has also been successfully utilized for LS⁷⁰.

An alternate icosahedral non-VLP platform is dihydrolipoyl acetyltransferase (E2p), an enzyme that assembles into a 60-mer hollow dodecahedron from 20 trimers and forms the core of the pyruvate dehydrogenase complex⁷¹. The E2p nanoparticle is slightly larger than LS (Table 1) and is able to present larger trimeric HIV surface antigens, such as full-length gp120 or gp140, through genetic fusion²². Attachment of the trimeric antigen to the nanoparticle increased B-cell stimulation compared to antigen alone. Antigens are fused at the N-terminus, which is located near the apex of the trimer, making it ideal for trimeric antigens, whereas the C-terminus (which is located at the dimeric interface between the trimers) is inaccessible.

The nonstructural protein 10 (nsp10) has recently gained interest as a nanoparticle due to its presence within the coronavirus genus, including the SARS-CoV-2 virus⁷². Nsp10 consists of 12 monomers that assemble into a spherical particle resembling a dodecamer with twelve faces. Both N- and C-terminals are surface-exposed and are located on separate threefold axes, which allows for the attachment of antigen, especially trimeric, to both terminals. Genetic fusion of nsp10 with a γ -herpesvirus antigen, gD, elicited binding antibody titers in rabbits⁷².

Smaller non-spherical particles have also been utilized. IMX313, a *Gallus gallus* ortholog of C4bp, forms a heptameric ring-like protein⁷³. The malaria antigen Pfs25 was fused to the N-terminal of IMX313, expressed in yeast, with vaccination resulting in significantly increased antibody titers compared to vaccination

with the antigen alone⁷³. A dual component, dual antigen IMX313 was also successfully developed through genetic fusion of SpyCatcher at the N-terminus and SnoopCatcher at the C-terminus, which was expressed in *E. coli* with refolding. The genetic fusions enabled attachments of two distinct malarial antigens Pfs25 and Pfs28 to IMX313 through coupling with SpyTag and SnoopTag, respectively⁴⁵. The multimeric antigens produced a significantly stronger antibody response than monomeric antigens.

Many highly oligomeric proteins have been successfully used as platforms. These proteins have distinct arrangements than their capsid VLP counterparts enabling unique nanoparticle presentation and design. Platforms such as Ferritin, LS, and E2p also contain a trimeric threefold favorable for the attachment of trimeric viral antigens such as the Spike protein of SARS-CoV-2. However, most of these self-assembling platforms are smaller in size than VLPs and may have only one terminus available for antigen attachment, which can limit the valency and compatibility for antigens.

Engineered nanoparticle platforms

Through rational or computational design, dimeric, trimeric, tetrameric, or pentameric proteins have been engineered to assemble into larger, highly oligomeric complexes that offer greater control over antigen stoichiometry, spacing, and particle size. These engineered particles present additional platforms for vaccines beyond the limited number of natural platforms. In order to develop novel platforms several methods and techniques of generating self-assembly have been developed. There are several design parameters for designing self-assembling proteins for use as a platform. First, the geometric symmetry and shape of the desired nanoparticle are determined by type of building blocks used. Second, self-assembly must be promoted by either fusing two different building blocks or engineering an interface between building blocks. Lastly, at least one terminal should be exposed and accessible for antigen attachment. Described below are the design and evolution of novel self-assembling proteins that have led to engineered platforms.

Coiled-coil-based protein design

Self-assembling peptide nanoparticles (SAPNs) are large protein assemblies composed of numerous coiled-coil domains. SAPNs are able to oligomerize into large icosahedral complexes because of interactions between individual coiled-coil domains. Formation of these complexes has been accomplished through the genetic fusion of a trimeric coiled-coil to a pentameric coiled-coil³⁴, and the utilization of a trimeric coiled-coil that binds to a dimeric coiled-coil⁷⁴. SAPNs are limited by the relatively small surface area of the monomeric building blocks. It is difficult to fuse large proteins to the monomers without them interfering with assembly, thus limiting the use of SAPNs to display small peptides or epitopes.

Tetrahedral protein design

Tetrahedral protein scaffolds were among the first to be explored⁷⁵ and optimized in 2012⁷⁶. Producing a tetrahedral platform requires the oligomerization of four trimeric building blocks (Fig. 4). One way of achieving this oligomerization is by engineering a dimeric interaction between two monomers of two separate trimers. The four trimers act as the vertices of a tetrahedron while the dimeric interactions serve to link the vertices (Fig. 4). In the **T3 + 2**⁷⁶ platform, oligomerization was achieved through a genetic fusion between a monomer of a trimer to a monomer of a dimer. This fusion allowed for the trimeric building blocks to self-assemble through the use of interconnecting dimers. Advances in the protein engineering

software Rosetta^{77,78} allowed for the creation of a single component tetrahedron, **T3**^{77,78}. By introducing a dimeric interface on the primary trimeric building block, the team removed the need for fusing a dimeric building block. The **T32**⁷⁸ design is similar to the **T3 + 2** design but with an engineered dimeric interface between the primary and secondary building blocks. In the **T33** design⁷⁸, four primary trimers act as the vertices of the tetrahedron and are joined together by secondary trimers aligned on the faces (Fig. 4), resulting in a two-component tetrahedral and octahedral nanoparticle.

Octahedral protein design

For octahedral designs, self-assembly is achieved through the linking of 8, primarily trimeric, building blocks with dimeric interactions. The **O3** design satisfied this criterion by using 8 trimeric building blocks with designed dimeric interfaces⁷⁷. Alternately, the genetic fusion of a trimer to a dimer using an alpha-helical linker resulted in an **O3 + 2** design⁷⁹. Both strategies produce cube-shaped nanoparticles, however, the fusion strategy led to polydisperse assemblies consisting of possible tetrahedrons and triangular prisms caused by the different possible symmetries that 3-folds with 2-folds can assemble into. A rigid-alpha linker was utilized to restrict the angle between the trimer and the dimer to drive octahedral assembly⁷⁹.

Although coiled-coil particles are limited to peptides, hybrid platforms developed may circumvent this limitation^{80,81}. Specifically, in the **O3 + 4CC** design, a trimeric protein used as the primary building block was fused to a tetrameric coiled coil, generating octahedron-like particles with tight packing between the trimeric faces and no discernable cavity, as seen on other engineered platforms due to the small secondary building block⁸⁰. An important design component was the linker length and flexibility between the primary and secondary building block and the most successful **O3 + 4CC** design produced octahedral assemblies with a homogeneity of 73.3%, determined by Analytical Ultracentrifugation⁸⁰.

Icosahedral protein design

In order to generate icosahedral self-assembly, either 20 trimeric vertices or 12 pentameric vertices must be linked together. One of the first icosahedral platforms, the **I3**, fulfills the first method⁸². It utilized a trimeric building block with an engineered dimeric interface to link the trimeric vertices together. The twenty trimers assemble to form a dodecahedron, with the trimeric building blocks aligned to the threefold vertices. Several two-component icosahedral platforms have been subsequently developed. The **I32**, notably, forms a dodecahedron similar to the **I3** platform but with a secondary dimeric building block inserted between the two trimers⁸³. By changing the primary building block to a pentameric one in an **I52** model, a platform resembling an icosahedron was created, with the pentameric building block aligning to the fivefold vertex and the secondary dimeric building blocks aligned to the edges⁸³. **I53** designs with a pentameric primary building block and a secondary trimeric building block were further developed⁸³. In this design, the pentameric building blocks were aligned with the vertices of an icosahedron, while the trimeric building blocks were aligned with the triangular faces to create assemblies resembling a rhombic triacontahedron (Fig. 4). Utilizing the same design template as the **I53** platform an icosahedral hybrid coiled-coil fusion platform, **I3 + 5CC** using a coiled-coil as the pentameric building block was produced⁸¹. The tight packing between the triangular faces causes the design to resemble an icosahedron rather than a rhombic triacontahedron. The triple component fusion design, **Ico532**, consists of a trimeric coiled coil fused with a flexible linker to a dimeric building block, which was rigidly fused to a pentameric building block⁸⁴. 60 monomers of the fusion protein assemble to form a structure

resembling an Icosahedron, similar to the **I52** (Fig. 4) structure but with the triangular cavities filled by the trimeric coiled-coils.

The design of self-assembling proteins has evolved from smaller, simpler, tetrahedral complexes to icosahedral complexes that rival the size of VLPs (Table 1). These designs contain symmetrical structures unseen in nature and yet to be explored as potential platforms. A notable difference for these novel proteins compared to natural proteins exists in their packing, with several designs (Fig. 4) featuring porous cavities, which arise due to the current limitations of generating self-assembly.

Some assembly required

The two strategies for generating self-assembly, fusion or engineered interfaces, each have their own advantages and disadvantages. Fusion is computationally less demanding but faces issues with non-specific assemblies, though several strategies have been developed to encourage uniform assemblies. Engineering interfaces have yielded homogeneous particles that has been successfully utilized as platforms. However, the low success rate of this strategy requires intensive screening of numerous designs.

The fusion strategy is rather straightforward: two monomers with different oligomeric stoichiometries are fused together. The two oligomerization domains must be held together rigidly else they may assemble irregularly⁷⁵. The use of a rigid alpha-helical linker connecting the helical termini of the building blocks mitigated the formation of heterologous assemblies^{75,76,79}. In addition, particular angles between a trimeric and dimeric building blocks were fused with a rigid linker that favors a certain symmetry⁷⁵. However, even with the optimized α -helical fusion, the octahedral cube **O3 + 2** has been shown to form tetrahedrons and triangular prisms⁷⁹. The hybrid coiled-coil **O3 + 4CC** designs also required linker optimization to achieve homogeneity⁸⁰. Initial designs utilized a trimeric primary building block fused to a dimeric coiled-coil building block through a flexible linker. This resulted in dimeric, tetrahedral, and octahedral complexes⁸⁵. Their octahedron design resulted in a significantly homogeneous population of proper complexes⁸⁰ while their icosahedron design resulted in a nearly homogenous population⁸¹. They observed that by varying the linker length between the primary and secondary building block, they were able to optimize homogeneity. The use of a fourfold and threefold in their **O3 + 4CC** and a fivefold and threefold in their **I3 + 5CC** may also restrict the oligomerization compared to less specific threefold and twofold combinations. This factor was taken into account with the **Ico532** design, although some heterologous assemblies still occurred. The design also contains an available trimeric N-terminus, which may be potentially used to genetically fuse antigens. In summary, optimizing linker length, reducing flexibility, and applying symmetry-based constraints should be taken into account for fusion strategies to reduce undesired assemblies.

Engineered interfaces follow similar geometric symmetry principles to the fusion strategy, but instead of fusing two oligomeric stoichiometries together it introduces another oligomeric binding site. The specificity of the engineered interface limits undesired assemblies, promoting the use of this strategy for platform development. GFP was successfully fused to the trimeric building block of the **T33-21** design, resulting in a nanoparticle displaying a total of 24 copies of GFP⁸². One or two GFP proteins were attached to **I3-01** through genetic fusion at the N- and C-terminus of the self-assembling protein⁸², though the N-terminal may be more suitable for antigen attachment due to the C-terminal being buried. A 19 kDa Designed ankyrin repeat protein (DARPin) was also successfully fused to **T33-21** using an α -helical linker⁸⁶ resulting in the presentation of 12 copies on the nanoparticle and enabling the small protein to be visualized by Cryo-EM. The **I3-01** nanoparticle has been fused to malarial

antigens using SpyCatcher-Spytag⁴³ in comparison with the AP205 VLP platform. Although **I3-01** presented less antigen, 60 compared to 180 in AP205, they both induced similar antibody levels. The **I3-01** design has also been genetically fused to a stabilized trimeric HIV envelope antigen gp140²³, with a ten amino acid length linker to account for the relatively large spacing of the N-termini. An alternative linker, which incorporated a T-cell epitope was also successfully incorporated. The trimeric antigen presented on **I3-01** generated significantly higher levels of antibodies compared to the trimeric antigen alone. Similarly, **I53-50** has been developed as an HIV vaccine, utilizing a prefusion trimer stabilized envelope antigen called SOSIP fused to the N-terminus of the trimeric secondary building block²⁴. Presentation of ConM genotype SOSIP trimers on **I53-50** demonstrated increased neutralizing antibody titers compared to SOSIP trimers alone. However, presentation of BG505 genotype SOSIP on **I53-50** elicited lower antibody titers and poorer neutralizing antibody response than BG505 SOSIP alone. This occurrence was attributed to less accessibility to the neutralizing epitopes of BG505, which were located at the base of the spike, due to attachment with the platform. However, further analysis demonstrated no change in antibody titers against other base-located epitopes with **I53-50** fused and non-fused SOSIP. Ultimately, this result suggests that it may be beneficial to orient antigen with neutralizing epitopes apically exposed. **I53-50** design has been utilized in a vaccine for respiratory syncytial virus (RSV)⁸⁷. A prefusion-stabilized variant of the RSV F glycoprotein trimer was fused to a trimeric foldon domain located at the N-terminus of the trimeric secondary building block. Neutralizing antibody titers induced by the antigen fused to **I53** were ten times greater than those that were induced by the trimeric antigen alone. **I53-50** has recently been utilized as a vaccine for SARS-CoV-2 with the Spike glycoprotein receptor-binding domain (RBD) genetically fused to the N-terminus of the trimeric building block with varying flexible linker lengths⁸⁸. In mice, immunizations with the RBD fused with **I53** designs generated a strong antibody response, while monomeric RBD failed to generate a detectable response, and stabilized prefusion Spike trimer (S-2P) elicited a weaker response. Similar results were seen in neutralizing antibody productions. RBD fused to **I53** was able to confer protection against SARS-CoV-2 replication while monomeric RBD and S-2P did not.

In conclusion, advancements in protein design have allowed for engineered platforms that have been successfully used in prototype vaccines. With comparable immunogenicity to natural platforms, these platforms surpass natural non-VLP platforms in size (Table 1) while having trimeric and dimeric-folds suitable for attachment of common trimeric and dimeric antigens. Furthermore, the two-component engineered-interface platforms allow for straightforward purification through controlled assembly. However, several limitations exist in the creation of engineered platforms such as heterogeneity with the fusion method and successful design yield with the engineered interface method. Strategies to alleviate heterogeneity will allow the use of fusion proteins as platforms. Improvements in structural prediction and interface design will increase the success rate of the engineered interface method and permit higher levels of packing. The development of new platforms and their design strategies will allow different configurations and a greater range of parameters to be examined and optimized for improved vaccine efficacy.

Critical parameters to consider for platform selection and design

Several factors such as size, antigen density, and surface properties are critical for the successful implementation of nanoparticles in vaccines. These parameters are described below in an attempt to guide the usage and development of platforms for improved immunogenicity. Although discrepancies may arise due to

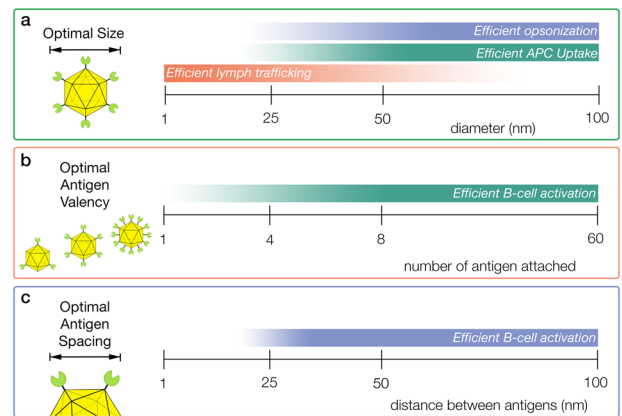


Fig. 5 Critical parameters of nanoparticle platforms and potential optimal ranges based on current research. Gradient increases in intensity from less optimal to most optimal. **a** Parameters for optimal size of a nanoparticle with a trend as size increases for enhanced opsonization and APC uptake, but inhibited lymph node trafficking. **b** Trend for improved B-cell activation as antigen valency increases. **c** The ideal range between antigen in order to facilitate efficient B-cell activation, with potential steric constraints preventing efficient B-cell activation at distances below 28 nm.

differences in nanoparticle composition the findings highlight mechanisms such as cellular uptake, opsonization, trafficking, and B-cell activation, that can be used to evaluate the performance of a platform.

Efficient cellular uptake, lymph follicle retention, and entry into lymph nodes are three critical factors that lead to improved immunogenicity and protection that is influenced by the size of a nanoparticle platform (Fig. 5a). Particles under 250 nm, which include most if not all protein platforms, utilize clathrin and scavenger receptor-dependent uptake pathways²⁵. Testing of polystyrene particles ranging from 40 to 1500 nm in diameter determined that particles below 500 nm had the highest uptake by dendritic cells⁸⁹. Specifically, polystyrene particles of 40, 100, and 500 nm all had relatively similar levels of uptake. Mathematical models have predicted the optimal size for cellular uptake to be between 20 and 30 nm⁹⁰. Spherical gold particles, conjugated to albumin as an antigen, had a lymph follicle retention time of 5 weeks with particles 50 and 100 nm in diameter compared to 48 h with particles 5 and 15 nm in diameter⁹¹. Furthermore, the larger particles were more likely to be presented on the FDC surface, allowing greater delivery of antigen to B-cells, and higher levels of B-cell maturation. Conversely, the smaller particles were able to enter the lymph node more rapidly than the larger particles. A similar result was seen with polypropylene sulfide nanoparticles, where particles 25 nm in diameter entered the lymph nodes 10 times more efficiently than 100 nm particles⁹². Thus, the optimal platform may be around 20–50 nm, large enough for efficient uptake and retention in lymph follicles, small enough for entry into the lymph node (Fig. 5a).

Optimal B-cell activation is dependent on the antigen valency and spacing (Fig. 5b, c). One study measured how valency affected B-cell activation through comparison of the monomeric engineered HIV gp120 antigen, eOD-GT, versus protein platforms with 4, 8, or 60 copies of eOD-GT⁹³. The 8-mer and 60-mer antigens demonstrated enhanced B-cell activation, B-cell proliferation and B-cell localization upon immunization of mice and this effect was not observed with lower valency antigens. Vaccination with the 60-mer also showed improved T-cell recruitment, IgG titers, and was able to rescue a low-affinity version of the antigen to induce B-cell differentiation. In contrast, examination of B-cells induced by 4-mer and 60-mer vaccinations revealed that the lower valency 4-mer had higher titers of B-cells binding to antigen probes,

suggesting that lower valency antigens generated higher affinity B-cells. However, differences in the angle and orientation with which the antigen was presented or other differences due to protein composition may have impacted the display of accessible epitopes. Additionally, differences between the protein platforms such as size, flexibility, and composition may also introduce confounding factors. In order to eliminate these factors a recent study used DNA origami platforms that could present antigens with defined valency and organization⁹⁴. The study compared valency using icosahedron shaped DNA platforms that presented 1, 2, 3, 5, 10, 30, or 60 copies of eOD-GT, with the benefits of increased valency on B-cell activation plateauing at 5. However, this result may have been hindered by inadequate antigen spacing. The study measured effects of antigen spacing between two antigens on a rod-shaped DNA platform with distances from 7 to 80 nm. B-cell activation increased as distance increased, plateaued at a distance of 28 nm and remained similarly elevated at 80 nm. The findings from this study suggest that steric constraints hinder BCR recruitment to antigen less than 30 nm apart (Fig. 5c).

Beyond size and structure other factors such as surface charge and hydrophobicity can influence the trafficking of particles and thus affect immunogenicity. Positively charged particles has been shown to promote uptake by macrophages and DCs due to electrostatic attraction to negatively charge membranes⁹⁵. On the other hand, hydrophobic particles have been shown to promote DC uptake, possibly through enhanced cell membrane interaction⁹⁶ or complement recruitment²⁶. However, the attachment of antigens can significantly change these surface properties, and thus it may be more appropriate to evaluate these properties in context of compatibility with the antigen. Further research is needed to comprehensively analyze how the surface charge and hydrophobicity of the platform affects trafficking and immune response.

These findings suggest the parameters for the ideal platform may be 20–50 nm in diameter with antigen spaced 30 nm apart. However, a more comprehensive study containing more particles with smaller intervals in size is needed for testing of uptake, opsonization, and lymph node trafficking. Furthermore, differences in particle composition may affect the results of size as well. A conclusive answer to the impact of valency will require testing of valencies with optimally spaced antigen. Antibody responses against the platform has been demonstrated in vaccines⁹⁷, which may potentially divert the humoral immune response from the antigen. Continued research and testing of more platforms are needed to determine the effects of this implication, as well as evaluate parameters for the development of more optimized platforms.

Future directions

Protein-based nanoparticles have demonstrated the ability to revolutionize vaccine development for various diseases. The design of optimal nanoparticles that effectively present antigens to produce the desired immune response is an active area of investigation. Computational design of nanoparticles has matured and allows for the expansion of available platforms for study. There are countless other possible building block arrangements that have yet to be explored as platforms. Additionally, all the engineered platforms share a common trait—a reliance on creating a dimeric interaction between the building blocks for self-assembly; more complicated symmetries may be investigated in the future. These approaches, along with more standardized methodology, are expected to contribute significantly to improving vaccines and alleviating the burden of global diseases.

DATA AVAILABILITY

No data were generated for the review article.

Received: 30 October 2020; Accepted: 22 March 2021;

Published online: 13 May 2021

REFERENCES

1. FDA. *Drug Products, Including Biological Products, that Contain Nanomaterials—Guidance for Industry*, <https://www.fda.gov/media/109910/download> (FDA, 2017).
2. Zhao, L. et al. Nanoparticle vaccines. *Vaccine* **32**, 327–337 (2014).
3. Song, C. et al. Recent advances in particulate adjuvants for cancer vaccination. *Adv. Therapeutics* **3**, 1900115 (2020).
4. Shin, H. et al. Recent advances in RNA therapeutics and RNA delivery systems based on nanoparticles. *Adv. Therapeutics* **1**, 1800065 (2018).
5. López-Sagaseta, J., Malito, E., Rappuoli, R. & Bottomley, M. J. Self-assembling protein nanoparticles in the design of vaccines. *Comput. Struct. Biotechnol. J.* **14**, 58–68 (2016).
6. Roldão, A., Mellado, M. C. M., Castilho, L. R., Carrondo, M. J. T. & Alves, P. M. Virus-like particles in vaccine development. *Expert Rev. Vaccines* **9**, 1149–1176 (2010).
7. Wu, Y., Narum, D. L., Fleury, S., Jennings, G. & Yadava, A. Particle-based platforms for malaria vaccines. *Vaccine* **33**, 7518–7524 (2015).
8. Pati, R., Shevtsov, M. & Sonawane, A. Nanoparticle vaccines against infectious diseases. *Front. Immunol.* **9**, 2224 (2018).
9. Yang, L. et al. Self-assembly of proteins: towards supramolecular materials. *Chem. A Eur. J.* **22**, 15570–15582 (2016).
10. Diaz, D., Care, A. & Sunna, A. Bioengineering strategies for protein-based nanoparticles. *Genes* **9**, 370 (2018).
11. Yeates, T. O. Geometric principles for designing highly symmetric self-assembling protein nanomaterials. *Annu. Rev. Biophys.* **46**, 23–42 (2017).
12. Kobayashi, N. & Arai, R. Design and construction of self-assembling supramolecular protein complexes using artificial and fusion proteins as nanoscale building blocks. *Curr. Opin. Biotechnol.* **46**, 57–65 (2017).
13. Luo, Q., Hou, C., Bai, Y., Wang, R. & Liu, J. Protein assembly: versatile approaches to construct highly ordered nanostructures. *Chem. Rev.* **116**, 13571–13632 (2016).
14. Bangaru, S. et al. Structural analysis of full-length SARS-CoV-2 spike protein from an advanced vaccine candidate. *Science* **370**, 1089 (2020).
15. Kaiser, C. R. et al. Biodistribution studies of protein cage nanoparticles demonstrate broad tissue distribution and rapid clearance in vivo. *Int. J. Nanomed.* **2**, 715–733 (2007).
16. Zinkernagel, R. M. On natural and artificial vaccinations. *Annu. Rev. Immunol.* **21**, 515–546 (2003).
17. Parker, D. C. T cell-dependent B cell activation. *Annu. Rev. Immunol.* **11**, 331–360 (1993).
18. Schiller, J. T. & Lowy, D. R. Understanding and learning from the success of prophylactic human papillomavirus vaccines. *Nat. Rev. Microbiol.* **10**, 681–692 (2012).
19. Liu, Y. V. et al. Chimeric severe acute respiratory syndrome coronavirus (SARS-CoV) S glycoprotein and influenza matrix 1 efficiently form virus-like particles (VLPs) that protect mice against challenge with SARS-CoV. *Vaccine* **29**, 6606–6613 (2011).
20. Brune, K. D. et al. Plug-and-display: decoration of Virus-Like Particles via isopeptide bonds for modular immunization. *Sci. Rep.* **6**, 19234 (2016).
21. Jardine, J. et al. Rational HIV immunogen design to target specific germline B cell receptors. *Science* **340**, 711 (2013).
22. He, L. et al. Presenting native-like trimeric HIV-1 antigens with self-assembling nanoparticles. *Nat. Commun.* **7**, 12041–12041 (2016).
23. He, L. et al. HIV-1 vaccine design through minimizing envelope metastability. *Sci. Adv.* **4**, eaau6769–eaau6769 (2018).
24. Brouwer, P. J. M. et al. Enhancing and shaping the immunogenicity of native-like HIV-1 envelope trimers with a two-component protein nanoparticle. *Nat. Commun.* **10**, 4272 (2019).
25. Jia, J. et al. Interactions between nanoparticles and dendritic cells: from the perspective of cancer immunotherapy. *Front. Oncol.* **8**, 404 (2018).
26. Bachmann, M. F. & Jennings, G. T. Vaccine delivery: a matter of size, geometry, kinetics and molecular patterns. *Nat. Rev. Immunol.* **10**, 787–796 (2010).
27. Irvine, D. J. & Read, B. J. Shaping humoral immunity to vaccines through antigen-displaying nanoparticles. *Curr. Opin. Immunol.* **65**, 1–6 (2020).
28. Bachmann, M. F. & Zinkernagel, R. M. Neutralizing antiviral B cell responses. *Annu. Rev. Immunol.* **15**, 235–270 (1997).
29. Jegerlehner, A. et al. Regulation of IgG antibody responses by epitope density and CD21-mediated costimulation. *Eur. J. Immunol.* **32**, 3305–3314 (2002).
30. Übelhart, R. et al. Responsiveness of B cells is regulated by the hinge region of IgD. *Nat. Immunol.* **16**, 534–543 (2015).

31. Krishnamachari, Y., Geary, S. M., Lemke, C. D. & Salem, A. K. Nanoparticle delivery systems in cancer vaccines. *Pharm. Res.* **28**, 215–236 (2011).
32. Takada, A. & Kawaoaka, Y. Antibody-dependent enhancement of viral infection: molecular mechanisms and in vivo implications. *Rev. Med. Virol.* **13**, 387–398 (2003).
33. Correia, B. E. et al. Proof of principle for epitope-focused vaccine design. *Nature* **507**, 201–206 (2014).
34. Karch, C. P. et al. The use of a *P. falciparum* specific coiled-coil domain to construct a self-assembling protein nanoparticle vaccine to prevent malaria. *J. Nanobiotechnology* **15**, 62 (2017).
35. Kaba, S. A. et al. Protective antibody and CD8⁺T-cell responses to the plasmodium falciparum circumsporozoite protein induced by a nanoparticle vaccine. *PLoS ONE* **7**, e48304 (2012).
36. Brune, K. D. & Howarth, M. New routes and opportunities for modular construction of particulate vaccines: stick, click, and glue. *Front. Immunol.* **9**, 1432 (2018).
37. Kelly, D. F., Moxon, E. R. & Pollard, A. J. Haemophilus influenzae type b conjugate vaccines. *Immunology* **113**, 163–174 (2004).
38. Shimp, R. L. et al. Development of a Pfs25-EPA malaria transmission blocking vaccine as a chemically conjugated nanoparticle. *Vaccine* **31**, 2954–2962 (2013).
39. Talaat, K. R. et al. Safety and immunogenicity of Pfs25-EPA/Alhydrogel[®], a transmission blocking vaccine against plasmodium falciparum: an open label study in malaria naïve adults. *PLoS ONE* **11**, e0163144–e0163144 (2016).
40. Sagara, I. et al. Safety and immunogenicity of Pfs25H-EPA/Alhydrogel, a transmission-blocking vaccine against Plasmodium falciparum: a randomised, double-blind, comparator-controlled, dose-escalation study in healthy Malian adults. *Lancet Infect. Dis.* **18**, 969–982 (2018).
41. Qian, F. et al. Conjugating recombinant proteins to *Pseudomonas aeruginosa* ExoProtein A: a strategy for enhancing immunogenicity of malaria vaccine candidates. *Vaccine* **25**, 3923–3933 (2007).
42. Leneghan, D. B. et al. Nanoassembly routes stimulate conflicting antibody quantity and quality for transmission-blocking malaria vaccines. *Sci. Rep.* **7**, 3811 (2017).
43. Bruun, T. U. J., Andersson, A.-M. C., Draper, S. J. & Howarth, M. Engineering a rugged nanoscaffold to enhance plug-and-display vaccination. *ACS Nano* **12**, 8855–8866 (2018).
44. Thrane, S. et al. Bacterial superglue enables easy development of efficient virus-like particle based vaccines. *J. Nanobiotechnol.* **14**, 30 (2016).
45. Brune, K. D. et al. Dual plug-and-display synthetic assembly using orthogonal reactive proteins for twin antigen immunization. *Bioconjugate Chem.* **28**, 1544–1551 (2017).
46. Zhang, B. et al. A platform incorporating trimeric antigens into self-assembling nanoparticles reveals SARS-CoV-2-spike nanoparticles to elicit substantially higher neutralizing responses than spike alone. *Sci. Rep.* **10**, 18149 (2020).
47. van den Berg, M., Ogotu, B., Sewankambo, N. K., Biller-Andorno, N. & Tanner, M. RTS,S malaria vaccine pilot studies: addressing the human realities in large-scale clinical trials. *Trials* **20**, 316 (2019).
48. Cohen, J., Nussenzweig, V., Vekemans, J. & Leach, A. From the circumsporozoite protein to the RTS,S/AS candidate vaccine. *Hum. Vaccines* **6**, 90–96 (2010).
49. Poland, G. A. & Jacobson, R. M. Prevention of hepatitis B with the hepatitis B vaccine. *N. Engl. J. Med.* **351**, 2832–2838 (2004).
50. Liang, T. J. Hepatitis B: the virus and disease. *Hepatology* **49**, S13–S21 (2009).
51. Mulder, A. M. et al. Toolbox for non-invasive structural and functional analysis of recombinant VLP based vaccines: a case study with hepatitis B vaccine. *PLoS ONE* **7**, e33235 (2012).
52. Collins, K. A., Snaith, R., Cottingham, M. G., Gilbert, S. C. & Hill, A. V. S. Enhancing protective immunity to malaria with a highly immunogenic virus-like particle vaccine. *Sci. Rep.* **7**, 46621–46621 (2017).
53. RTS, S Clinical Trials Partnership. Efficacy and safety of RTS,S/AS01 malaria vaccine with or without a booster dose in infants and children in Africa: final results of a phase 3, individually randomised, controlled trial. *Lancet* **386**, 31–45 (2015).
54. Liu, Y. V. et al. Recombinant virus-like particles elicit protective immunity against avian influenza A(H7N9) virus infection in ferrets. *Vaccine* **33**, 2152–2158 (2015).
55. McCraw, D. M. et al. Structural analysis of influenza vaccine virus-like particles reveals a multicomponent organization. *Sci. Rep.* **8**, 10342 (2018).
56. Wang, D. et al. The lack of an inherent membrane targeting signal is responsible for the failure of the matrix (M1) protein of influenza A virus to bud into virus-like particles. *J. Virol.* **84**, 4673 (2010).
57. Buffin, S. et al. Influenza A and B virus-like particles produced in mammalian cells are highly immunogenic and induce functional antibodies. *Vaccine* **37**, 6857–6867 (2019).
58. Deo, V. K., Kato, T. & Park, E. Y. Chimeric virus-like particles made using GAG and M1 capsid proteins providing dual drug delivery and vaccination platform. *Mol. Pharmaceutics* **12**, 839–845 (2015).
59. Tissot, A. C. et al. Versatile virus-like particle carrier for epitope based vaccines. *PLoS ONE* **5**, e9809 (2010).
60. Shishovs, M. et al. Structure of AP205 coat protein reveals circular permutation in ssRNA bacteriophages. *J. Mol. Biol.* **428**, 4267–4279 (2016).
61. Palladini, A. et al. Virus-like particle display of HER2 induces potent anti-cancer responses. *Oncol Immunology* **7**, e1408749 (2018).
62. Lua, L. H. L. et al. Bioengineering virus-like particles as vaccines. *Biotechnol. Bioeng.* **111**, 425–440 (2014).
63. Lu, Y., Chan, W., Ko, B. Y., VanLang, C. C. & Swartz, J. R. Assessing sequence plasticity of a virus-like nanoparticle by evolution toward a versatile scaffold for vaccines and drug delivery. *Proc. Natl Acad. Sci. USA* **112**, 12360 (2015).
64. Hempstead, P. D. et al. Comparison of the three-dimensional structures of recombinant human H and horse L ferritins at high resolution. *J. Mol. Biol.* **268**, 424–448 (1997).
65. Sun, W. et al. Salt-dependent aggregation and assembly of *E. coli*-expressed ferritin. *Dose-Response* **14**, 1559325816632102–1559325816632102 (2016).
66. Yao, D. et al. Human H-ferritin presenting RBM of spike glycoprotein as potential vaccine of SARS-CoV-2. Preprint at *bioRxiv* <https://doi.org/10.1101/2020.05.25.115618> (2020).
67. Kanekiyo, M. et al. Self-assembling influenza nanoparticle vaccines elicit broadly neutralizing H1N1 antibodies. *Nature* **499**, 102–106 (2013).
68. Georgiev, I. S. et al. Two-component ferritin nanoparticles for multimerization of diverse trimeric antigens. *ACS Infect. Dis.* **4**, 788–796 (2018).
69. Zhang, X., Meining, W., Fischer, M., Bacher, A. & Ladenstein, R. X-ray structure analysis and crystallographic refinement of lumazine synthase from the hyperthermophile Aquifex aeolicus at 1.6Å resolution: determinants of thermostability revealed from structural comparisons. *J. Mol. Biol.* **306**, 1099–1114 (2001).
70. Ra, J.-S., Shin, H.-H., Kang, S. & Do, Y. Lumazine synthase protein cage nanoparticles as antigen delivery nanopatforms for dendritic cell-based vaccine development. *Clin. Exp. Vaccin. Res.* **3**, 227–234 (2014).
71. Izard, T. et al. Principles of quasi-equivalence and Euclidean geometry govern the assembly of cubic and dodecahedral cores of pyruvate dehydrogenase complexes. *Proc. Natl Acad. Sci. USA* **96**, 1240–1245 (1999).
72. Carter, D. C., Wright, B., Jerome, W. G., Rose, J. P. & Wilson, E. A unique protein self-assembling nanoparticle with significant advantages in vaccine development and production. *J. Nanomater.* **2020**, 4297937 (2020).
73. Li, Y. et al. Enhancing immunogenicity and transmission-blocking activity of malaria vaccines by fusing Pfs25 to IMX313 multimerization technology. *Sci. Rep.* **6**, 18848 (2016).
74. Mosayebi, M. et al. Beyond icosahedral symmetry in packings of proteins in spherical shells. *Proc. Natl Acad. Sci. USA* **114**, 9014 (2017).
75. Padilla, J. E., Colovos, C. & Yeates, T. O. Nanohedra: Using symmetry to design self assembling protein cages, layers, crystals, and filaments. *Proc. Natl Acad. Sci. USA* **98**, 2217 (2001).
76. Lai, Y.-T., Cascio, D. & Yeates, T. O. Structure of a 16-nm cage designed by using protein oligomers. *Science* **336**, 1129 (2012).
77. King, N. P. et al. Computational design of self-assembling protein nanomaterials with atomic level accuracy. *Science* **336**, 1171 (2012).
78. King, N. P. et al. Accurate design of co-assembling multi-component protein nanomaterials. *Nature* **510**, 103–108 (2014).
79. Lai, Y.-T. et al. Structure of a designed protein cage that self-assembles into a highly porous cube. *Nat. Chem.* **6**, 1065–1071 (2014).
80. Sciore, A. et al. Flexible, symmetry-directed approach to assembling protein cages. *Proc. Natl Acad. Sci. USA* **113**, 8681 (2016).
81. Cristie-David, A. S. et al. Coiled-coil-mediated assembly of an icosahedral protein cage with extremely high thermal and chemical stability. *J. Am. Chem. Soc.* **141**, 9207–9216 (2019).
82. Hsia, Y. et al. Design of a hyperstable 60-subunit protein icosahedron. *Nature* **535**, 136–139 (2016).
83. Bale, J. B. et al. Accurate design of megadalton-scale two-component icosahedral protein complexes. *Science* **353**, 389 (2016).
84. Cannon, K. A., Nguyen, V. N., Morgan, C. & Yeates, T. O. Design and characterization of an icosahedral protein cage formed by a double-fusion protein containing three distinct symmetry elements. *ACS Synth. Biol.* **9**, 517–524 (2020).
85. Patterson, D. P. et al. Characterization of a highly flexible self-assembling protein system designed to form nanocages. *Protein Sci.* **23**, 190–199 (2014).
86. Liu, Y., Gonen, S., Gonen, T. & Yeates, T. O. Near-atomic cryo-EM imaging of a small protein displayed on a designed scaffolding system. *Proc. Natl Acad. Sci. USA* **115**, 3362 (2018).
87. Marcandalli, J. et al. Induction of potent neutralizing antibody responses by a designed protein nanoparticle vaccine for respiratory syncytial virus. *Cell* **176**, 1420–1431. e17 (2019).
88. Walls, A. C. et al. Elicitation of potent neutralizing antibody responses by designed protein nanoparticle vaccines for SARS-CoV-2. *Cell* **183**, 1367–1382. e17 (2020).
89. Foged, C., Brodin, B., Frokjaer, S. & Sundblad, A. Particle size and surface charge affect particle uptake by human dendritic cells in an in vitro model. *Int. J. Pharmaceutics* **298**, 315–322 (2005).

90. Chaudhuri, A., Battaglia, G. & Golestanian, R. The effect of interactions on the cellular uptake of nanoparticles. *Phys. Biol.* **8**, 046002 (2011).
91. Zhang, Y.-N. et al. Nanoparticle size influences antigen retention and presentation in lymph node follicles for humoral immunity. *Nano Lett.* **19**, 7226–7235 (2019).
92. Reddy, S. T. et al. Exploiting lymphatic transport and complement activation in nanoparticle vaccines. *Nat. Biotechnol.* **25**, 1159–1164 (2007).
93. Kato, Y. et al. Multifaceted effects of antigen valency on B cell response composition and differentiation in vivo. *Immunity* **53**, 548–563 (2020).
94. Veneziano, R. et al. Role of nanoscale antigen organization on B-cell activation probed using DNA origami. *Nat. Nanotechnol.* **15**, 716–723 (2020).
95. Kwon, Y. J., Standley, S. M., Goh, S. L. & Fréchet, J. M. J. Enhanced antigen presentation and immunostimulation of dendritic cells using acid-degradable cationic nanoparticles. *J. Controlled Release*. **105**, 199–212 (2005).
96. Liu, Y. et al. Surface hydrophobicity of microparticles modulates adjuvanticity. *J. Mater. Chem. B Mater. Biol. Med.* **1**, 3888–3896 (2013).
97. Lainšček, D. et al. Immune response to vaccine candidates based on different types of nanoscaffolded RBD domain of the SARS-CoV-2 spike protein. Preprint at *bioRxiv* <https://doi.org/10.1101/2020.08.28.244269> (2020).
98. Catalan, E. Mémoire sur la théorie des polyèdres. *J. l'École Polytechnique* **24**, 1–71 (1865).
99. Scriba, C. J. The six-cornered snowflake, by Johannes Kepler. Edited and translated by Colin Hardie, with essays. *Can. Math. Bull.* **12**, 107–107 (1969).

ACKNOWLEDGEMENTS

This work was supported by the Intramural Research Program of the National Institute of Allergy and Infectious Diseases, National Institutes of Health. The authors thank Palak Patel, Thayne Dickey, Nichole Salinas, Dashuang Shi and J. Patrick Gorres for constructive comments and edits to the manuscript.

AUTHOR CONTRIBUTIONS

N.H.T. and B.N. conceived manuscript. B.N. wrote the first draft of the manuscript and N.H.T. edited, reviewed, and approved the manuscript.

FUNDING INFORMATION

Open Access funding provided by the National Institutes of Health (NIH).

COMPETING INTERESTS

The authors declare no competing interests.

ADDITIONAL INFORMATION

Correspondence and requests for materials should be addressed to NirajH. Tolia

Reprints and permission information is available at <http://www.nature.com/reprints>

Publisher's note Springer Nature remains neutral with regard to jurisdictional claims in published maps and institutional affiliations.



Open Access This article is licensed under a Creative Commons Attribution 4.0 International License, which permits use, sharing, adaptation, distribution and reproduction in any medium or format, as long as you give appropriate credit to the original author(s) and the source, provide a link to the Creative Commons license, and indicate if changes were made. The images or other third party material in this article are included in the article's Creative Commons license, unless indicated otherwise in a credit line to the material. If material is not included in the article's Creative Commons license and your intended use is not permitted by statutory regulation or exceeds the permitted use, you will need to obtain permission directly from the copyright holder. To view a copy of this license, visit <http://creativecommons.org/licenses/by/4.0/>.

This is a U.S. Government work and not under copyright protection in the US; foreign copyright protection may apply 2021, corrected publication 2021